Gap equations for the p- and d-channels of pairing have the identical form

$$\frac{1}{\lambda_l} = \frac{1}{N} \sum_p \frac{|\psi_l(p)|^2}{2E_{pl}} \tanh \frac{E_{pl}}{2T}, \tag{3}$$

where E_{pl} is the usual BCS-type gap excitation spectrum, but despite this similarity the solutions of Eqn (3) for the p- and t-type pairing behave differently.

The reason for this stems from the angular dependences of $|\psi_l(p)|^2$. Was the gap isotropic, the main contribution to the integral over the Brillouin zone would be determined by the narrow energy region near the van Hove singularity. For a d-type gap, the angular dependence acts to maintain the large van Hove-singularity contribution, whereas in the p-channel case the angular dependence is such as to cancel the singularity. For this reason, the numerical solution of Eqn (3) yields $T_c(\mathrm{p}) \ll T_c(\mathrm{d})$ even for $\lambda_p = \lambda_d$ (Fig. 5). Thus, for optimally doped cuprates and ruthenates, where typically $\lambda_p = \lambda_d = 0.5$ and $t = 0.1$ eV, one finds $T_c(\mathrm{p}) \approx 2.5$ K and $T_c(\mathrm{d}) \approx 70$ K.

This work has been supported by the Krasnoyarsk regional Science Foundation through Grant No. 8F0032.

References

1. Ginzburg V L, Maksimov E G *Sverkhprovodimost* **5** 1543 (1992) [*SPCT* **5** 1505 (1992)]
2. Dagotto E *Rev. Mod. Phys.* **66** 763 (1994)
3. Shen Z X, Dessaw D S *Phys. Rep.* **253** 1 (1995)
4. Loktev V M *Fiz. Nizk. Temp.* **22** 3 (1996) [*Low Temp. Phys.* **22** 1 (1996)]
5. Ovchinnikov S G *Usp. Fiz. Nauk* **167** 1043 (1997) [*Phys. Usp.* **40** 993 (1997)]
6. Bianconi A et al. *Physica C* **162–164** 209 (1990)
7. Romberg H et al. *Phys. Rev. B* **41** 2609 (1990)
8. Ovchinnikov S G, Sandalov I S *Physica C* **161** 607 (1989)
9. Gavrichkov V A, Ovchinnikov S G *Fiz. Tverd. Tela* (St. Petersburg) **40** 184 (1998) [*Phys. Solid State* **40** 163 (1998)]
10. Jefferson J H *Physica B* **165–166** 1013 (1990)
11. Lovtsov S V, Yushankhai V Yu *Physica C* **179** 159 (1991)
12. Jefferson J H, Eshes H, Feiner L F *Phys. Rev. B* **45** 7959 (1992)
13. Zhang F C, Rice T M *Phys. Rev. B* **37** 3759 (1988)
14. Feiner L F, Jefferson J H, Raimondi R *Phys. Rev. B* **53** 8751 (1996)
15. Feiner L F, Jefferson J H, Raimondi R *Phys. Rev. B* **53** 8774 (1996)
16. Kamimura H, Eto M J *Jpn. J. Phys. Soc.* **59** 3053 (1990)
17. Eshes H, Tjeng L H, Sawatzky G A *Phys. Rev. B* **41** 288 (1990)
18. Ovchinnikov S G *Pis'ma Zh. Eksp. Teor. Fiz.* **64** 23 (1996) [*JETP Lett.* **64** 25 (1996)]
19. Zaĭtsev R O *Zh. Eksp. Teor. Fiz.* **70** 1100 (1976) [*Sov. Phys. JETP* **44** 652 (1976)]
20. Wells B O et al. *Phys. Rev. Lett.* **74** 964 (1995)
21. Ovchinnikov S G *Zh. Eksp. Teor. Fiz.* **102** 534 (1992) [*Sov. Phys. JETP* **75** 283 (1992)]
22. Marshall D S et al. *Phys. Rev. Lett.* **76** 4841 (1996)
23. Avramov P V, Ovchinnikov S G *Zh. Strukt. Khim.* **40** 131 (1999)
24. Scalapino D J *Phys. Rep.* **250** 329 (1995)
25. Izyumov Yu A *Usp. Fiz. Nauk* **169** 225 (1999) [*Phys. Usp.* **42** 215 (1999)]
26. Wu D H et al. *Phys. Rev. Lett.* **70** 85 (1993)
27. Stadlober B et al. *Phys. Rev. Lett.* **74** 4911 (1995)
28. Rice T M, Sirist M *J. Phys.: Condens. Matter* **7** 643 (1995)
29. Akhiezer A I, Pomeranchuk I Ya *Zh. Eksp. Teor. Fiz.* **36** 859 (1959) [*Sov. Phys. JETP* **9** 605 (1959)]
30. Kuz'min E V, Ovchinnikov S G, Baklanov I O *Zh. Eksp. Teor. Fiz.* **116** 655 (1999) [*JETP* **89** 349 (1999)]
31. Plakida N M, Yushankhai V Yu, Stasyuk I V *Physica C* **160** 80 (1989)

PACS numbers: **74.25.–q**, **74.72–h**
DOI: 10.1070/PU2000v043n02ABEH000708

Experimental studies of the thermal and electronic properties of $Ba_{1-x}K_xBiO_3$ and other perovskite-like oxide HTSC systems

A I Golovashkin, A P Rusakov

The basic properties of the cuprate high-temperature superconductors (HTSC) are attributed to the antiferromagnetic (AF) ordering of Cu ions known as the spin density wave (SDW). Recently, however, a number of anomalies have been discovered which cannot be explained by this ordering mechanism alone. To provide an insight into their origin, the noncuprate HTSC systems $Ba_{1-x}K_xBiO_3$ (BKBO) and $BaPb_xBi_{1-x}O_3$ (BPBO) showing similar anomalies have been studied in this work.

Neutron diffraction studies have shown that doping causes a strong softening of the high-frequency portion of the BKBO phonon spectra [1]. The analysis of the dispersion curves $\omega(\mathbf{Q})$ has further shown that in the metallic phase of an HTSC the high-frequency longitudinal optical phonons $\omega_{\mathrm{LO}}(\mathbf{Q})$ are soften anomalously strongly on doping [2–4]. For wave vectors $\mathbf{Q}$ near the boundary of the Brillouin zone, the frequencies $\omega_{\mathrm{LO}}(\mathbf{Q})$ become lower than the transverse optical frequencies $\omega_{\mathrm{TO}}(\mathbf{Q})$ ('ω_{LO} anomaly'). For all the HTSCs investigated — BKBO, $La_{2-x}Sr_xCuO_4$ (LSCO), and $YBa_2Cu_3O_{7-x}$ (YBCO) — the anomalous dispersion of ω_{LO} was observed only along [100] and never along other directions, in particular [110]. Notice here that if AF ordering was the dominant ordering mechanism along [110], there would necessarily be ω_{LO} anomalies in the same direction, which is not the case experimentally.

We have shown that for the BKBO, BPBO [5, 6], and LSCO [7] systems at low temperatures T the linear expansion coefficient $\alpha(T)$ is anomalous (negative). This effect is observed only in high-quality samples. Similar anomalies have also been seen in YBCO [8] and Bi-2219 [9]. In single-crystal samples of LSCO, YBCO, and Bi-2212, $\alpha(T)$ is anisotropic — the less so, the higher the doping level.

An interesting point about the HTSC systems is the anomalously strong magnetic-field dependence of the thermal expansion, $\alpha(H)$. Up to 4 T, the region of negative values of α is observed to shrink, while at the same time moving towards lower temperatures in both cuprate and copper-free HTSCs [10].

Optical measurements reveal that while the energy gap between the valence band and the conduction band in the BKBO and BPBO systems narrows with doping, it still remains observable even in the metallic phase, provided the material is moderately doped [11–14]. Evidence for this has also been seen in LSCO using the ultrahigh-resolution (7 MeV) photoelectron emission method [15, 16] and in Bi-2212 using an X-ray absorption technique [17]. Thus, the 'metallic' phase is that of a degenerate semiconductor both for copper-free and cuprate HTSCs.

Another common anomaly of HTSC systems is the existence of EPR signals in the 'half field' with a g factor of about 4. This 'forbidden' signal is observed in the presence of localized triplet pairs. The absorption line with $g \approx 4.2$ (in addition to that with $g \approx 2.1$) was observed in EPR absorption measurements on high-quality BKBO and BPBO

samples over a wide range of their compositions [18]. Similar signals were also seen in LSCO [19] and YBCO [20].

The fact that [100] is a preferred direction in HTSC systems, both cuprate and copper-free, also manifests itself in the shape of their Fermi surfaces. It has been found experimentally that large portions of the Fermi surface in BKBO [21], Bi-2212 [22], YBCO [23], and other HTSCs are parallel to the [100] directions rather than [110] as one would expect was AF the only ordering mechanism for the Cu ions.

Thus, experiment shows that both the phonon and electronic spectra of the cuprate and copper-free HTSC systems are influenced by the fact that the [100] directions are the preferred ones. We are clearly faced here with a conflict between the body of experimental data and theoretical models which include only ordering along the [110] directions of a metallic sublattice (charge ordering $Bi^{+3}-Bi^{+5}$ in BKBO, and AF ordering $Cu\uparrow-Cu\downarrow$ in the cuprates). To resolve the problem, let us discuss the experimental data on the electronic and structural properties of the HTSC systems.

High-resolution X-ray [24] and neutron diffraction [25] studies on high-quality single crystals of BKBO have revealed that the lattice parameter along the [100] directions is doubled and that such unit cells with double the value of lattice parameter have four oxygen ions whose valence is lower than that of the others. The analysis of data on doping, together with the condition of charge neutrality, imply that the $BaBiO_3$ and BKBO compounds in the dielectric state for $x \leqslant 0.25$ are described by the chemical formulas

$$Ba_8^{+2}Bi_4^{+3}(Bi_4^{+3.5}O_4^{-0.5})O_{20}^{-2}$$

and

$$Ba_{8-8x}^{+2}K_{8x}^{+1}Bi_4^{+3+2x}(Bi_4^{+3.5}O_4^{-0.5})O_{20}^{-2}\,,$$

respectively [26]. In the metallic phase ($x \geqslant 0.25$), BKBO is described by

$$Ba_{8-8(0.25+y)}^{+2}K_{8(0.25+y)}^{+1}Bi_4^{+3.5}(Bi_4^{+3.5}O_4^{-0.5})O_{20}^{-2} + 8y\,,$$

where $8y$ is the hole concentration ($0 \leqslant y \leqslant 0.25$; the maximum value of y is determined by the solubility of potassium: $Ba_{0.5}K_{0.5}BiO_3$ for the ordinary nondoubled unit cell). Thus, the doubled BKBO unit cell possesses four 'covalent' bonds $Bi-O^{-0.5}$ in addition to the 'ionic' bonds $Bi-O^{-2}$. The ordering of these bonds in the metallic ($x > 0.25$) phase is illustrated in Fig. 1a, which shows that covalent bonds are ordered in mutually perpendicular [100] directions in the neighboring BiO_2 layers — the type of ordering that models real charge density waves (CDW) in the oxygen ion sublattice.

Recent inelastic neutron scattering studies [4] have shown for the specific case of LSCO at $T \approx 10$ K that there are two groups of $Cu-O$ bonds in the CuO_2 plane, which can be termed, somewhat loosely, as 'covalent' and 'ionic,' and whose ordering in the [100] directions results in the doubling of the lattice parameters in the CuO_2 plane. It is through this ordering that a CDW in the oxygen sublattice of the cuprate HTSCs manifests itself. For YBCO, such ordering was observed for $T \leqslant 35$ K [27]. From the analysis of the Hall effect (μSR) and neutron diffraction studies [26] it follows that the ordered $La_{2-x}Sr_xCuO_4$ lattice may be represented by

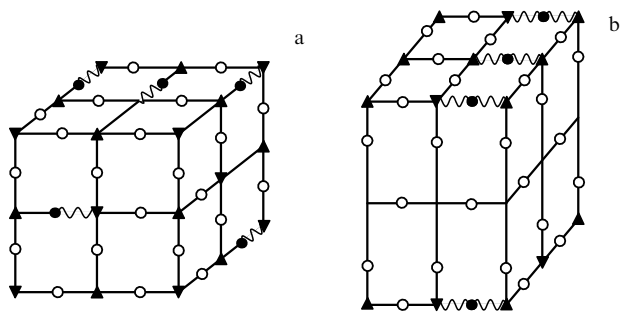

Figure 1. Unit cells with a doubled lattice parameter. (a) BKBO: ▲, ▼, Bi ions of different valency ($x < 0.25$); ○, O^{-2}; •, $O^{-0.5}$; wavy line represents the covalent $Bi-O^{-0.5}$ bond. Ions of Ba and K are not shown. Covalent bonds in neighboring BiO_2 layers are ordered in mutually perpendicular [100] directions. (b) LSCO: ▲, ▼, Cu ions with up and down spins; ○, O^{-2}; •, $O^{-1.5}$; wavy line shows the $Cu-O^{-1.5}$ covalent bond. Covalent bonds in neighboring CuO_2 layers are ordered in mutually perpendicular [100] directions. Ions of La and Sr are not shown.

the following chemical formula

$$La_{8(2-x)}^{+3}Sr_{8x}^{+2}(Cu_8^{+1.75}O_4^{-1.5})O_{28}^{-2} + 8x\,,$$

where $8x$ ($0 \leqslant x \leqslant 0.25$) is the concentration of hole carriers. Thus, by analogy with BKBO, the doubled unit cell of LSCO contains four 'covalent' bonds $Cu-O^{-1.5}$. Their ordering is shown in Fig. 1b, where covalent bonds are seen to be ordered in mutually perpendicular [100] directions in neighboring CuO_2 layers.

Applying a similar analysis to $YBa_2Cu_3O_7$ yields the formula [26]

$$(Cu_4^{+1.5}O_4^{-1})Ba_8^{+2}Y_4^{+3}(Cu_8^{+1.75}O_4^{-1.5})O_{28}^{-2} + 2h\,,$$

where $2h$ is the hole concentration. The $Cu_8^{+1.75}O_4^{-1.5}$ block specified in the formula is common to all the layered cuprate HTSCs and accounts for the similarity in their physical properties.

The importance of charge ordering in the oxygen sublattice and the type of this ordering were predicted in our earlier work [28] and have been confirmed directly in recent experimental work [4, 24, 27].

For a doubled BKBO unit cell, the Brillouin zone is a cube reduced to half its size (Fig. 2a, dashed line). Two electrons from four $O^{-0.5}$ ions fill the first Brillouin zone, and nesting on the reciprocal lattice vector $\mathbf{G} = (\pi/a)$ [100] results in the formation of an insulating gap $\Sigma \approx 2$ eV at low levels of potassium doping. Potassium doping produces hole carriers near the top of the valence band, which when they go degenerate produce a hole Fermi surface (the region of hole states is hatched in Fig. 2a) with planes parallel to the (100) cube edges. Estimations of the Fermi surface agree well with experiment for $Ba_{0.6}K_{0.4}BiO_3$ as shown in Fig. 2a.

For cuprate HTSCs, the first (flat) Brillouin zone is also reduced by half as in BKBO, but the unit cell now has four $O^{-1.5}$ ions, with the consequence that the first three Brillouin zones are filled (the boundary of the third zone is represented by a dashed line in Fig. 2b). Nesting on the vector $\mathbf{G} = (\pi/a)$ [100] leads to an insulating gap $\Sigma \approx 2$ eV along the boundary of the third filled Brillouin zone. Scattering on the vector (π/a) [110] gives an additional contribution to the magnitude of Σ. As the material is

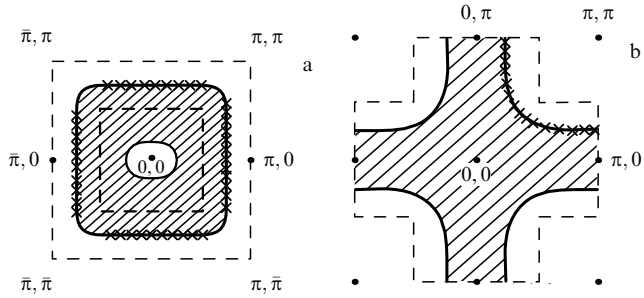

Figure 2. Fermi surface of oxide HTSCs. (a) $Ba_{0.6}K_{0.4}BiO_3$, cross section in the plane $k_z = 0$. The hatched region is that of the hole states near the boundary of the reduced Brillouin zone. Solid line, prediction of Ref. [26]; crosses, experiment [21]. (b) A layered cuprate compound. Dashed line, the boundary of the third Brillouin zone for the doubled unit cell; solid line, predicted Fermi surface; crosses, experiment on $Bi_2Sr_2CaCu_2O_8$ [29]. Region of electron-filled states is shown hatched.

doped and carriers become degenerate, a Fermi surface is formed, which is schematically shown by the solid line in Fig. 2b. The experimental data of Ref. [29] (crosses) agree well with estimates. As in BKBO, flat areas of the Fermi surface parallel to the [100] directions are observed.

As seen in Fig. 2, the nesting conditions also hold (i.e. areas parallel to [100] exist) for not too high doping concentrations, which is the reason for the anomalies in some of the physical properties of the HTSCs. Nesting $E(\mathbf{k}+\mathbf{G}) = E(\mathbf{k})$ onto the vector $\mathbf{G} = (\pi/a)$ [100] results in a discontinuity of the electron susceptibility $\chi(\mathbf{Q}) \sim [E(\mathbf{k}+\mathbf{Q}) - E(\mathbf{k})]^{-1}$ for $\mathbf{Q} = \mathbf{G}$ and $|\mathbf{k}| \to |\mathbf{G}|/2$ [30]. This implies that the dielectric constant of the electron subsystem,

$$\varepsilon(\mathbf{Q}) = 1 + \frac{(4\pi e^2/|\mathbf{Q}|^2)|\chi(\mathbf{Q})|}{1 - (4\pi e^2/|\mathbf{Q}|^2)L(\mathbf{Q})|\chi(\mathbf{Q})|}\,,$$

decreases below zero [31] for $\mathbf{Q} \approx \mathbf{G}$. Further, since at the high-frequency end of the longitudinal phonon mode $\omega_{\mathrm{LO}}^2(\mathbf{Q}) \approx \omega_{\mathrm{TO}}^2(\mathbf{Q}) + (\omega_{\mathrm{p}}^*)^2/\varepsilon(\mathbf{Q})$ [32], it follows that for $\varepsilon(\mathbf{Q}) < 0$ we have $\omega_{\mathrm{LO}}^2 \approx \omega_{\mathrm{TO}}^2 - (\omega_{\mathrm{p}}^*)^2/|\varepsilon(\mathbf{Q})| < \omega_{\mathrm{TO}}^2$. Here ω_{p}^* is the ion plasma frequency, and $\omega_{\mathrm{TO}}(\mathbf{Q})$ is the frequency of the transverse short-wavelength optical phonon mode, which is practically independent of $\mathbf{Q}$ in cuprates. Thus, the ω_{Lo} re-screening anomaly arises from the nesting along [100], which in turn is due to the appearance of CDWs in the oxygen sublattice.

The electronic structure discussed above gives a clue to the $\alpha(T)$ anomaly. Since the electronic structure of the system is unstable initially, the system undergoes reconstruction accompanied by doubling of its lattice constant. In the initial system we can write $\omega_{\mathrm{TA}}^2 < 0$ formally [33]. After the reconstruction, the system is stable due to the appearance of a nonuniform density distribution (CDW) in the oxygen sublattice, the stabilization effect ($\omega_{\mathrm{TA}}^2 > 0$) being due to the additional Coulomb interaction between the CDW and the lattice ions. As T increases, so does the amplitude of ion oscillations, which increases the overlap of their electronic shells thus increasing the screening of the charges. As a result, the CDW amplitude (A_{CDW}) decreases and the system becomes less stable ($\omega_{\mathrm{TA}}^2 \to 0$). The thermal expansion anomaly should be observed in the region $kT \sim \hbar\omega_{\mathrm{TA}}(\mathbf{Q} \approx \mathbf{G})$. As T is further increased, other $\mathbf{Q} \neq \mathbf{G}$ phonons are excited thus making thermal expansion normal.

The magnetic field H influences thermal expansion by decreasing A_{CDW} [30]. Since this should cause a decrease in ω_{TA}, the region of instability ($\alpha < 0$) is expected to shift towards lower temperatures — which is precisely what one observes experimentally.

The EPR signal with $g \approx 2.1$ in BKBO and BPBO is due to imperfections (defects) in the ideal ordering of covalent $\mathrm{Bi-O}^{-0.5}$ bonds. Such defects have a localized magnetic moment and 'show up' in EPR measurements. The coupled pairs of such defects produce a singlet ground state and a triplet excited state [18], of which the latter is seen as an anomalous EPR signal in a 'half field' with $g \approx 4.2$. Ordinary defects act to 'wash out' this line. The $g \approx 4.2$ signal is also observed in cuprate HTSCs, but in these the strong EPR line of Cu^{+2} ions has a masking effect.

The most important 'anomaly' of the HTSCs — the high critical temperature T_{c} — relates, in our view, to the peculiarities of their electronic structure, which have been discussed above. We spoke, in particular, of re-screening $\omega_{\mathrm{LO}}^2 < \omega_{\mathrm{TO}}^2$ for $\mathbf{Q} \approx \mathbf{G}$. In this case the dielectric constant $\varepsilon(\mathbf{Q} \to \mathbf{G}) < 0$. The negative values of $\varepsilon(\mathbf{Q} \approx \mathbf{G})$ cause the pairing of electrons via phonons with $\mathbf{Q} \approx \mathbf{G}$, a process which creates electron pairs with a coherence length $\xi \sim 1/|\mathbf{G}|$ and produces a pseudogap at the Fermi surface. Such pairs form a Bose–Einstein condensate as their concentration increases. As can be seen from Fig. 2, the congruent (flat) [100]-parallel portions of the Fermi surface secure a high density of states. Given the phonon frequency $\omega_{\mathrm{LO}} \sim 70-90$ meV, critical temperatures $T_{\mathrm{c}} \sim 100$ K are readily achieved. Thus we see that electron pairing in HTSCs is dominated by short-wave bosons. Notice also that close to the point $(\pi/2, \pi/2)$ of the Brillouin zone, the reduction of the phase space region results in the narrowing of the superconducting gap Δ in the [110] directions or, in other words, the gap becomes strongly anisotropic.

In conclusion, we believe that the CDW in the oxygen sublattice is the main reason for the anomalies observed in HTSCs, both bismuthate- and cuprate-based. There is convincing experimental evidence to show that

— in addition to the ordering in the metal sublattice, HTSCs also exhibit ordering (CDW) in the oxygen ion sublattice in the [100] direction. The consequences of this ordering are the doubled lattice parameter, a new Brillouin zone, nesting on the vector (π/a) [100], and the dielectric ground state; the insulating gap is due to the presence of the CDW and SDW, i.e. due to oxygen sublattice ordering which appears in addition to that in the metal (Bi, Cu) sublattice.

— introducing doping gives rise to a Fermi surface with flat portions parallel to [100], implying that the nesting conditions still apply for relatively low doping.

— nesting on the vector $\mathbf{G} = (\pi/a)$ [100] results in a divergent susceptibility $\chi(\mathbf{Q})$ and a negative $\varepsilon(\mathbf{Q})$ for $\mathbf{Q} \approx \mathbf{G}$; the negative dielectric constant $\varepsilon(\mathbf{Q})$ is the reason for the $\omega_{\mathrm{LO}}(\omega_{\mathrm{LO}} < \omega_{\mathrm{TO}})$ anomaly for vectors $\mathbf{Q} \approx \mathbf{G}$ in the [100] direction.

— a CDW in the oxygen sublattice and the additional CDW-induced interaction with the ions adds stability to the lattice, so that $\omega_{\mathrm{TA}}(\mathbf{Q} \approx \mathbf{G}) > 0$; heating the material causes the CDW amplitude to decrease because of the screening effect, thus leading to a smaller ω_{TA}, i.e. to the compression of the crystal. The magnetic field also reduces the CDW amplitude and ω_{TA} and shifts the region of anomalous (negative) thermal expansion towards lower temperatures.

This research was supported by the Superconductivity Research Council as part of the Russian Scientific and Technology Program 'Topical Problems in Condensed Matter Physics'. We gratefully acknowledge the cooperation of N V Anshukova, S V Gudenko, L I Ivanova, K V Kraĭskaya, I B Krynetskiĭ, L I Leonyuk, and A Yu Yakubovskiĭ in conducting the experiments.

References

1. Zemlyanov M G et al. *Physica B* **174** 360 (1991); *Physica C* **185–189** 1367 (1991)
2. Braden M et al. *J. Supercond.* **8** 595 (1995)
3. Reichardt W et al. *J. Supercond.* **7** 399 (1994)
4. McQueeney R J et al. *Phys. Rev. Lett.* **82** 628 (1999)
5. Anshukova N V et al. *J. Supercond.* **7** 427 (1994)
6. Anshukova N V et al. *Int. J. Modern Phys. B* **12** 3251 (1998)
7. Anshukova N V et al. *Physica C* **282–287** 1065 (1997)
8. You H, Welp U, Fang Y *Phys. Rev. B* **43** 3660 (1991)
9. Yang Z J et al. *J. Supercond.* **8** 223 (1995)
10. Golovashkin A I et al. *Physica B* (in press)
11. Uchida S, Kitazawa K, Tanaka S *Phase Transitions* **8** 95 (1987)
12. Blanton S H et al. *Phys. Rev. B* **47** 996 (1993)
13. Karlow M A et al. *Phys. Rev. B* **48** 6499 (1993)
14. Puchkov A V et al. *Phys. Rev. B* **54** 6686 (1996)
15. Ino A et al. *Phys. Rev. Lett.* **81** 2124 (1998)
16. Sato T et al. *Phys. Rev. Lett.* **83** 2254 (1999)
17. Ghigna P et al. *Phys. Rev. B* **57** 13426 (1998)
18. Yakubovskiĭ A Yu et al. *Zh. Eksp. Teor. Fiz.* **115** 1326 (1999) [*JETP* **88** 732 (1999)]
19. Kochelaev B I et al. *Phys. Rev. Lett.* **79** 4274 (1997)
20. Eremina R M et al. *Physica B* (in press)
21. Mosley W D et al. *Phys. Rev. Lett.* **79** 4274 (1997)
22. Marshall D S et al. *Phys. Rev. Lett.* **76** 4841 (1996)
23. Matsuura A et al. *Phys. Rev. B* **55** 2796 (1997)
24. Du C H et al. *J. Phys.: Condens. Matter* **6** L575 (1994)
25. Lightfoot P et al. *J. Solid State Chem.* **92** 473 (1991)
26. Golovashkin A I et al. *Physica C* **317–318** 630 (1999)
27. Krämer S, Mehring M *Phys. Rev. Lett.* **83** 396 (1999)
28. Anshukova N V et al. *Prog. High-Temper. Supercond.* **32** 403 (1992)
29. Ding H et al. *Phys. Rev. Lett.* **78** 2628 (1997)
30. Kopaev Yu V *Tr. Fiz. Inst. Akad. Nauk SSSR* **86** 3 (1975)
31. Maksimov E G *Tr. Fiz. Inst. Akad. Nauk SSSR* **86** 101 (1975)
32. Rice M J, Wang Y R *Physica C* **157** 192 (1989)
33. Maksimov E G, in *Problemy Vysokotemperaturnoĭ Sverkhprovodimosti* (The Problems of High-Temperature Superconductivity) (Eds V L Ginzburg, D A Kirzhnits) (Moscow: Nauka, 1977) Chs 3, 4 [Translated into English: *High-Temperature Superconductivity* (Eds V L Ginzburg, D A Kirzhnits) (New York: Consultants Bureau, 1982)]